Dear Editors and Referees,

On behalf of all co-authors, I would like to thank you for allowing us to revise our manuscript. We are very grateful for the editors' and referees' careful evaluation, as well as for the constructive and encouraging comments on our manuscript.

We have carefully considered all comments and suggestions and have revised the manuscript accordingly. All corresponding changes have been highlighted in red in the revised manuscript. Below, we provide a point-by-point response to each comment, with our replies marked in blue. We have made every effort to address the concerns raised and to improve the quality and clarity of the manuscript.

Please find the revised version attached for your kind consideration. We greatly appreciate the time and effort you and the referees have devoted to evaluating our work, and we look forward to your further feedback.

Thank you and best regards.

Responds to the referees' comments:

Referee #1:

Comments:

The paper is quite boastful and ignores the complexities of projecting VIIRS global nighttime light back to 1992. Earth Observation Group provides access to the DMSP monthly nighttime lights from 1992-2021 and VIIRS from 2012-2025. EOG's offerings are clearly the first open-access time series of monthly nighttime lights spanning 1992-2025. DMSP and VIIRS nighttime lights differ from each other in several key ways: A) VIIRS DNB pixel footprints are 42+ times smaller than DMSP. Many small lights detected by VIIRS are absent in DMSP. B) VIIRS has lower detection limits and a wider dynamic range. In contrast, DMSP nighttime light observations use 6-bit quantization and frequently saturate in bright city centers. C) The VIIRS overpass time is typically between midnight and 03:00 local time. The early DMSP record (1992-2013) had mid-evening overpass times, between 19:30 and 21:30. The DMSP extension series (2013-2021) has pre-dawn overpass times. Nighttime lights have variable diurnal patterns. This paper's data from 1992 to 2011 are speculative and cannot be recommended for quantitative use. The earliest VIIRS data are from 2012. The paper's title is thus misleading. The paper takes an ill-informed and swaggering approach to generating monthly nighttime lights from 1992-2011.

Response: Thank you for your comments. Although we agree with the proposed point to a certain degree, we still firmly believe our dataset contributes to existing nighttime light products and will have wide applications for its unique characteristics. Below is our detailed response.

First, we acknowledge that the monthly nighttime light products released by the Earth Observation Group (EOG) serve as an important base for studies with long-term global nighttime lights. Essentially, our dataset was built upon the EOG products, which are explicitly cited and discussed in our manuscript (see page 4, lines 120–123 in the revised manuscript, corresponding to lines 113–117 in the original version). Despite that, it is worth noting that our dataset was improved compared

to existing global nighttime light products, including the EOG datasets. Existing archives from EOG do not provide a consistent monthly nighttime light time series spanning 1992–2025. Instead, the available DMSP (1992–2021) and VIIRS (2012–present) monthly datasets originate from different sensors, exhibiting substantial discrepancies in spatial resolution, radiometric characteristics, as well as observation conditions. Specifically, the lack of VIIRS-like 500m resolution monthly data prior to 2012 hinders the construction of a temporally consistent long-term time series. To bridge this gap, we developed a super-resolution modeling framework to reconstruct a VIIRS-like monthly nighttime light dataset (approximately 500 m) for 1992–2024. To our knowledge, the developed dataset represents the longest monthly nighttime light time series at 500m resolution. We also commit to integrating future VIIRS releases to ensure the dataset's continued relevance. As suggested, to avoid potential ambiguity caused by the original title, we have rephrased it as "A Temporally Consistent Global 500 m-Resolution Monthly VIIRS-Like Nighttime Light Dataset (1992–2024)", of which the contributions of our work were highlighted.

Second, we also agree that the DMSP and VIIRS data differ in several crucial aspects, and these differences have been explicitly mitigated in our reconstruction framework as follows:

(A) We addressed the spatial resolution discrepancy using a deep super-resolution framework that transforms DMSP data into VIIRS-like products. Building on previous successes in annual NTL reconstruction (Chen et al., 2024, 2021; Cui et al., 2026; Zhang et al., 2024), our model enhances coarse 1 km DMSP data to a 500 m resolution. Crucially, in response to the observation that DMSP often fails to detect small light sources visible to VIIRS, we incorporated Landsat reflectance and impervious surface data as auxiliary constraints. This strategy allows the network to "fill in" missing spatial information beyond the DMSP sensor's detection limit. The theoretical feasibility of this multi-source fusion approach is further elaborated in Section 3 (Methodology).

(B) To reconcile discrepancies in dynamic range and saturation, we employ radiometric correction and multi-task learning strategies. While previous studies (Chen et al., 2024, 2021) have modeled the relationship between saturated DMSP observations and the wider radiometric range of VIIRS through pixel-level learning strategies, primarily by minimizing Mean Squared Error (MSE). As such, we extend this foundation to further improve the radiometric consistency between these two sensors. Specifically, our framework augments the conventional MSE-based objective with harmonized fitting constraints and frequency-domain alignment. As detailed in Section 3.3 and formulated in Eq. (12), this integrated approach enables a more robust reconstruction of nighttime light intensity across an expanded dynamic range.

$$\mathcal{L}_{\text{reg}} = \text{MSE}(\text{pred},\ \text{gt}) + \left(1 - L_{\text{fitness}}(\text{pred},\ \text{gt})\right) + L_1(|\text{FFT}(\text{pred})|,\ |\text{FFT}(\text{gt})|) \qquad (12)$$

where $pred$ denotes the reconstructed VIIRS values and gt represents the VIIRS reference. This design enables the deep learning model to more effectively transform the saturated DMSP values within the 0–63 range into a VIIRS-like radiometric space, while simultaneously constraining the two nighttime light datasets to maintain consistent overall temporal trends.

The additional content incorporated into Figs. 8 (page 15), 19, and 20 (page 23) in the revised manuscript (see below) further illustrates how the proposed dataset mitigates saturation and blooming effects in the original DMSP data. The additional panel in Fig. 8(d) quantitatively illustrates the radiometric differences between the original DMSP data and the super-resolved VIIRS-like outputs across different DMSP DN levels. It also includes a statistical analysis of pixels

with DN = 63, showing that more than 16% of these saturated pixels are mapped to higher simulated values. The examples at the top of Fig. 8 further demonstrate that the super-resolved data can effectively enhance the spatial resolution of nighttime lights. The visual comparisons in Figs. 19 and 20 provide additional evidence that the proposed dataset yields a more refined representation of nighttime light patterns in selected urban regions.

Figs. 8 (page 15), 19, and 20 (page 23) in the revised manuscript:

"

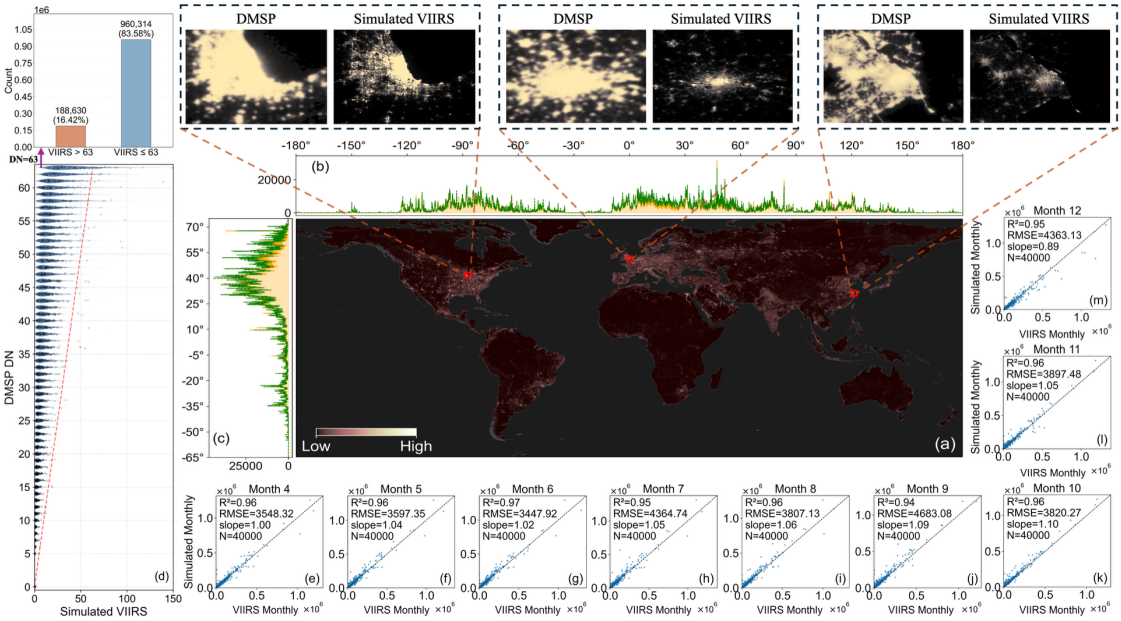

Figure 8. The simulated VIIRS-like data. **(a)** The generated global NTL intensity in 2012. **(b)** The longitudinal and **(c)** latitudinal sum of VIIRS NTL (orange) and Predicted VIIRS (green) with 1° bin (unit: nW cm^{-2} sr^{-1}). **(d)** Distribution of simulated VIIRS NTL across DMSP DN levels. **(e)** to **(m)** illustrate the city-level prediction errors of the total monthly VIIRS-like NTL from April to December 2012 at the global scale (unit: nW cm^{-2} sr^{-1}).

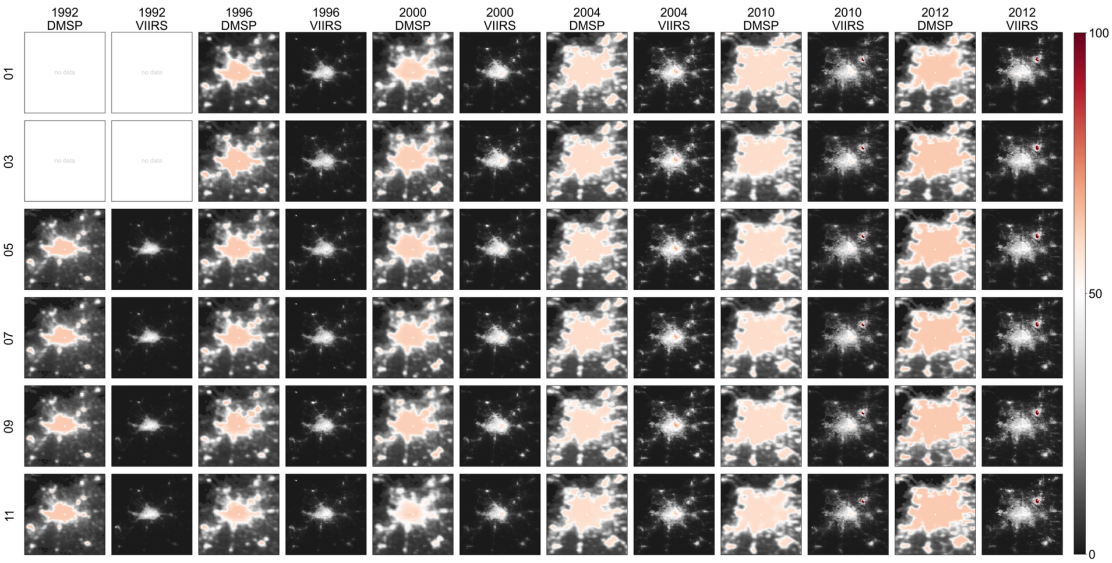

Figure 19. Seasonal and interannual spatial patterns of DMSP and reconstructed VIIRS-like NTL in Beijing from 1992 to 2012.

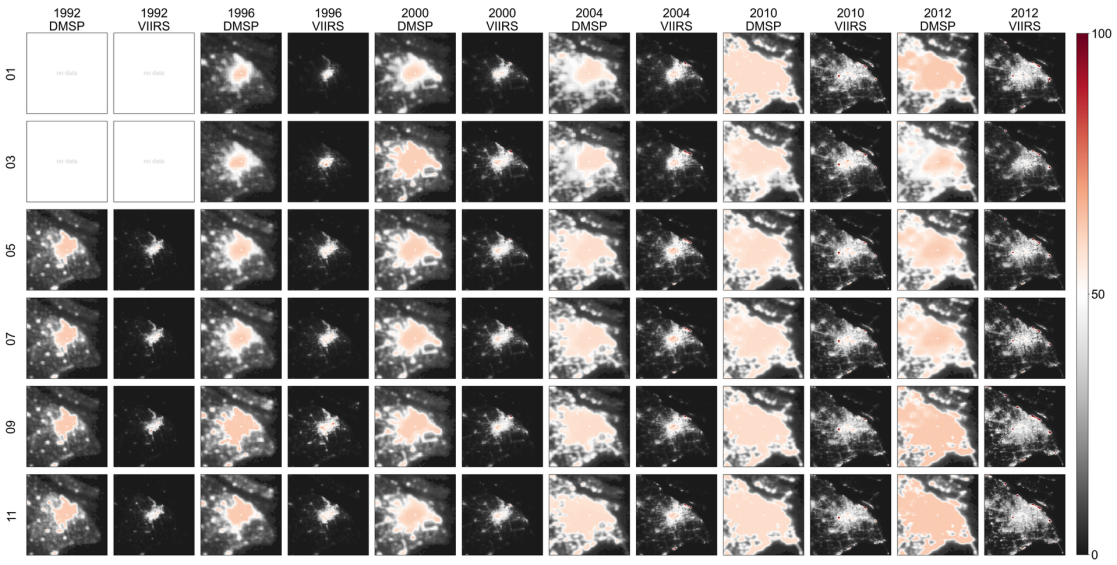

Figure 20. Seasonal and interannual spatial patterns of DMSP and reconstructed VIIRS-like NTL in Shanghai from 1992 to 2012."

(C) Regarding the discrepancy in overpass time between DMSP and VIIRS, we acknowledge that diurnal variability in nighttime lights may introduce systematic differences between the two sensors. Nevertheless, the relative temporal stability of urban infrastructure lighting, such as streetlights, provides a physical basis for cross-sensor alignment. In this study, to reduce the systematic bias associated with differences in overpass time, we implemented a temporal calibration strategy based on the overlapping observation period, using 2013 as the training year for the NightNet deep learning model. Through its nonlinear modeling capability, the model can learn stable cross-sensor relationships across differing observation conditions and thereby mitigate temporal inconsistencies caused by overpass-time differences. Similar attempts have also been explored by the Earth Observation Group, which employed deep learning to address discrepancies between DMSP and VIIRS. However, their approach converted VIIRS observations into DMSP-like products, namely the DMSP-like Nighttime Lights Derived from VNL (DVNL) (Nechaev et al., 2021).

Furthermore, we applied month-by-month forward and backward temporal corrections (as shown on page 13, lines 423–431 in the revised manuscript; corresponding to page 12, lines 407–415 in the original manuscript) to refine the consistency of the super-resolved results. Our validation confirms the efficacy of this approach: the reconstructed data show high agreement with VIIRS measurements during the overlapping months in 2012 (R^2 = 0.65 and RMSE = 14.27 at the pixel scale, R^2 = 0.96 at the city scale, as shown in Figs. 9, 13, and 14). Evaluations against radiance-calibrated DMSP products (1996, 1999, 2000, 2003, 2006, and 2010) further verify the reconstruction accuracy, with R^2 consistently exceeding 0.94, as shown in Fig. 16. These results demonstrate that our framework effectively minimizes overpass-related differences to produce a harmonized long-term time series.

References:

1. Baugh, K., Elvidge, C. D., Ghosh, T., and Ziskin, D.: Development of a 2009 Stable Lights Product using DMSP-OLS data, Proc. Asia-Pac. Adv. Netw., 30, 114, https://doi.org/10.7125/apan.30.17, 2010.

2. Chen, X., Wang, Z., Zhang, F., Shen, G., and Chen, Q.: A global annual simulated VIIRS nighttime light dataset from 1992 to 2023, Sci. Data, 11, 1380, https://doi.org/10.1038/s41597-024-04228-6, 2024.
3. Chen, Z., Yu, B., Yang, C., Zhou, Y., Yao, S., Qian, X., Wang, C., Wu, B., and Wu, J.: An extended time series (2000–2018) of global NPP-VIIRS-like nighttime light data from a cross-sensor calibration, Earth Syst. Sci. Data, 13, 889–906, https://doi.org/10.5194/essd-13-889-2021, 2021.
4. Cipolla, R., Gal, Y., and Kendall, A.: Multi-task Learning Using Uncertainty to Weigh Losses for Scene Geometry and Semantics, in: 2018 IEEE/CVF Conference on Computer Vision and Pattern Recognition, 2018 IEEE/CVF Conference on Computer Vision and Pattern Recognition (CVPR), 7482–7491, https://doi.org/10.1109/CVPR.2018.00781, 2018.
5. Cui, Y., Shi, G., Zhao, C., Li, Q., Yao, H., and Guo, W.: A global continuous 500 m nighttime light dataset (1992–2024) via NDVI-guided DMSP-OLS correction and U-TransNet cross-sensor harmonization, Int. J. Appl. Earth Obs. Geoinformation, 148, 105230, https://doi.org/10.1016/j.jag.2026.105230, 2026.
6. Ding, L. and Goshtasby, A.: On the Canny edge detector, Pattern Recognit., 34, 721–725, https://doi.org/10.1016/S0031-3203(00)00023-6, 2001.
7. Elvidge, C. D.: Mapping City Lights With Nighttime Data from the DMSP Operational Linescan System, Photogramm. Eng. Remote Sens., 63, 727–734, 1997.
8. Li, X. and Zhou, Y.: A Stepwise Calibration of Global DMSP/OLS Stable Nighttime Light Data (1992–2013), Remote Sens., 9, 637, https://doi.org/10.3390/rs9060637, 2017.
9. Li, X., Zhou, Y., Zhao, M., and Zhao, X.: A harmonized global nighttime light dataset 1992–2018, Sci. Data, 7, 168, https://doi.org/10.1038/s41597-020-0510-y, 2020.
10. Nechaev, D., Zhizhin, M., Poyda, A., Ghosh, T., Hsu, F.-C., and Elvidge, C.: Cross-Sensor Nighttime Lights Image Calibration for DMSP/OLS and SNPP/VIIRS with Residual U-Net, Remote Sens., 13, 5026, https://doi.org/10.3390/rs13245026, 2021.
11. Woo, S., Park, J., Lee, J.-Y., and Kweon, I. S.: CBAM: Convolutional Block Attention Module, in: Computer Vision – ECCV 2018: 15th European Conference, Munich, Germany, September 8–14, 2018, Proceedings, Part VII, Munich, Germany, 3–19, https://doi.org/10.1007/978-3-030-01234-2_1, 2018.
12. Zhang, C., Mao, Z., Nie, J., Lai, Y., and Deng, L.: A Comparative Study of Deep Learning Methods for Super-Resolution of Npp-Viirs Nighttime Light Images, https://doi.org/10.2139/ssrn.5017152, 2024.

Referee #2:

Comments:

This study addresses a crucial demand in nighttime light (NTL) remote sensing research by developing a long-term, high-resolution monthly VIIRS-like NTL dataset (MVNL) for 1992–2024, and the research work is of great scientific value and practical significance. Fusing multi-source NTL data to extend the temporal coverage of high-resolution products is an inevitable and essential approach to studying long-term urbanization and socioeconomic dynamics over the past decades, despite inherent limitations from the spatiotemporal inconsistencies of original DMSP-OLS and NPP-VIIRS data. This study makes prominent contributions to the field: it constructs the first 500 m-resolution monthly VIIRS-like NTL dataset spanning 1992–2024, filling the gap of high-resolution (500 m) multi-source fused long-term NTL products (only 1 km-resolution products are currently available); the reconstructed dataset achieves high consistency with existing EOG products (R^2=0.96 at city scale for overlapping months in 2012, R^2=0.98 at city scale for 2012 annual composite), and is further verified against radiance-calibrated DMSP products (R^2>0.94 at city

scale), demonstrating high reliability for city-level applications; additionally, the dataset has been freely shared online, providing a valuable and accessible data resource for global urbanization, socioeconomic analysis and related cross-disciplinary research. Overall, the research design is rigorous, the technical route is feasible, and the data product has important application prospects. I recommend the manuscript for minor revision and subsequent acceptance. Specific revision suggestions are as follows:

Comment #1: Since there are already existing attempts at 1 km-resolution long-term NTL products, the title "The World's First Long-Term Global 500 m-Resolution Monthly VIIRS Nighttime Lights Dataset (1992–2024)" may have certain ambiguities. It is necessary to clearly specify whether the dataset is the world's first 500 m-resolution product, the first global-scale product, or the first monthly-scale product, so as to avoid misunderstandings by readers.

Response: Thank you. To avoid potential ambiguity caused by the title, we rephrased it accordingly. Although the proposed dataset, to our knowledge, represents the first long-term global monthly VIIRS-like NTL product at 500 m resolution spanning 1992–2024, we acknowledge that the use of "first" may lead to misunderstandings due to varying interpretations. Therefore, we have modified the title to "A Temporally Consistent Global 500 m-Resolution Monthly VIIRS-Like Nighttime Light Dataset (1992–2024)" to improve clarity and avoid ambiguity.

Comment #2: The DMSP data covers 1992 to 2013, while the NPP-VIIRS data covers 2012 to the present, with the overlapping years of the two datasets being 2012 and 2013. It is advisable to clearly state these overlapping years in the abstract, and explicitly explain that the 2012 NPP-VIIRS data was used as the validation dataset in the study design. Otherwise, readers may be confused about why the validation accuracy is based on 2012 data.

Response: Thank you for this insightful comment. In our revised manuscript, we explicitly state in the abstract that the overlapping years between the DMSP and NPP-VIIRS datasets are 2012 and 2013. Meanwhile, we also clarify that the 2012 NPP-VIIRS data were used as an independent validation dataset in our study.

"Leveraging multi-modal observations, monthly VIIRS-like products are reconstructed by translating calibrated DMSP data from 1992 to 2013, with 2012 and 2013 serving as the overlapping years between the DMSP and NPP-VIIRS datasets. In particular, the 2013 annual data were used for model training and cross-sensor mapping, and the 2012 monthly NPP-VIIRS data were used as an independent validation benchmark. To construct the long-term VIIRS-like time series, we additionally gap-filled missing observations in the monthly NPP-VIIRS data for 2012–2024 and performed temporal correction to the reconstructed 1992-2012 NTL using the monthly NPP-VIIRS data from 2012 to 2013."

Comment #3: The abstract mentions using 2013–2024 VIIRS data as a reference to reconstruct 1992–2013 DMSP data. However, from the technical perspective, the reconstruction primarily uses the 2013 VIIRS data (the overlapping year) to establish the model. It is necessary to more clearly describe how the 2013–2024 VIIRS data is used as a reference for DMSP data reconstruction. For example, if my understanding is correct, the 2013 data is mainly used to establish the NightNet model, while the 2013–2024 time series data is mainly used to correct the temporal variation trend

of DMSP data.

Response: Thank you for the comment. The 2012-2024 NPP-VIIRS data were used for gap-filling of missing VIIRS observations, model development and validation, and temporal calibration of the VIIRS-like dataset. **Specifically,** monthly data from 2012 to 2024 were first used to fill missing observations and generate a fixed monthly VIIRS dataset. **Next,** the 2013 annual data were used for model training and cross-sensor mapping, while the 2012 monthly data served as an independent validation benchmark. **Finally,** the 2012-2013 monthly data were used to temporally correct the reconstructed VIIRS-like time series for 1992–2012. In the revised abstract, we have clarified the different roles of the VIIRS data in the reconstruction framework.

"Leveraging multi-modal observations, monthly VIIRS-like products are reconstructed by translating calibrated DMSP data from 1992 to 2013, with 2012 and 2013 serving as the overlapping years between the DMSP and NPP-VIIRS datasets. In particular, the 2013 annual data were used for model training and cross-sensor mapping, and the 2012 monthly NPP-VIIRS data were used as an independent validation benchmark. To construct the long-term VIIRS-like time series, we additionally gap-filled missing observations in the monthly NPP-VIIRS data for 2012–2024 and performed temporal correction to the reconstructed 1992-2012 NTL using the monthly NPP-VIIRS data from 2012 to 2013."

Comment #4: Supplement the detailed methodological principles of the joint intra-annual and inter-annual interpolation strategy mentioned in Line 205 (used for gap-filling the 1992–2012 monthly DMSP series), as the current manuscript only mentions the application of the strategy but lacks a clear explanation of its core principles, which affects the reproducibility of the research.

Response: Thanks for the insightful suggestion. To improve reproducibility, we have revised the manuscript to provide a more lucid and detailed description of the joint intra- and inter-annual interpolation strategy. The workflow follows a hierarchical approach: First, the intra-annual interpolation is applied to fill data gaps in a target month by leveraging temporal similarities among available observations within the same year, where missing regions are estimated using information from other available months of that year, thereby helping preserve within-year temporal variability as much as possible. Subsequently, for months that remain entirely missing or heavily fragmented, inter-annual interpolation is applied using observations from corresponding months in neighboring years to ensure long-term continuity. By synergistically integrating these two steps, the framework effectively maintains both fine-scale seasonal variability and robust inter-annual consistency in the reconstructed DMSP series (see Section 3.1, page 7, lines 212–223).

Revised statement:

"The preprocessing workflow began with the reconstruction of monthly DMSP observations from EOG, which initially contained extensive missing pixels and even entire months missing in several years. To generate a temporally continuous input for the subsequent cross-sensor enhancement, we implemented a joint intra-annual and inter-annual interpolation strategy to reconstruct a gap-filled monthly DMSP series from 1992 to 2012, as illustrated in Fig. 3. Specifically, for monthly images with partial missing areas, intra-annual interpolation was first conducted by exploiting the temporal similarity among adjacent months within the same year. The missing regions in a target month were estimated using the average information from other available months of that year, so that the seasonal pattern within the annual cycle could be preserved as much as possible.

For months that were completely missing or still contained substantial gaps after the intra-annual step, inter-annual interpolation was further conducted by referring to the corresponding month or temporally adjacent months in neighboring years, thereby preserving long-term temporal continuity across years. By combining these two procedures, the method simultaneously accounts for seasonal variability within each year and temporal consistency across successive years, enabling the construction of a continuous monthly DMSP time series for subsequent modeling."

Comment #5: For the complex algorithms involved in the spatiotemporal fusion model constructed in this study, clearly distinguish existing mature algorithms/models and the original algorithms of this study. For the adopted existing algorithms, add relevant reference citations and briefly explain the reasons for selection (e.g., core advantages, wide and successful application in remote sensing data spatiotemporal fusion); for the use of existing programs, provide a brief description as well.

Response: Thanks for the comment. The proposed spatiotemporal fusion framework and NightNet were not directly adapted from any single existing mature network architecture or ready-made model. Instead, the model was independently developed for cross-sensor VIIRS-like NTL reconstruction, while being informed by widely used deep learning principles in image reconstruction and remote sensing applications. The originality of this study lies in the task-specific integration of these principles into a unified framework for DMSP-to-VIIRS reconstruction, together with the design of dedicated modules for cross-sensor alignment, contextual enhancement, and synergistic structural supervision (Sections 3.2.1–3.2.3). To better demonstrate the effectiveness of our method, we further supplemented comparative experiments with several representative baseline networks and reported their performance in the revised manuscript (pages 14 and 15, lines 467–477). These results quantitatively demonstrate the advantages of our method.

Supplementary experiments:

"**Table 1.** Quantitative comparison of the proposed method with baseline networks

Method	Params. (M)	FLOPs (G)	PSNR	SSIM	R^2
FCN	1.18	1.10	46.89	0.9676	0.3817
UNet	0.79	51.49	46.37	0.9623	-
DeepLabv3+	40.34	17.26	50.44	0.9877	0.4878
HRNet	18.80	7.30	46.42	0.9620	-
NightNet	9.21	9.80	52.42	0.9930	0.8078

A comparison between NightNet and several widely used representative baseline networks, including FCN (Long et al., 2015), UNet (Ronneberger et al., 2015), DeepLabv3+ (Chen et al., 2018), and HRNet (Wang et al., 2021), was conducted to evaluate the effectiveness of the proposed architecture and clarify the rationale for its design. The quantitative results in terms of model complexity and reconstruction performance are presented in Table 1. As shown, our NightNet achieves the best overall performance, with the highest PSNR (52.42), SSIM (0.9930), and R^2 (0.8078), indicating superior reconstruction accuracy and structural consistency. Although some baseline models, such as DeepLab v3+, also show relatively strong performance, their results remain inferior to those of NightNet. Moreover, the DeepLab v3+ model has more model parameters (40.34M parameters) than NightNet (9.21M), yet yields lower reconstruction accuracy. The result indicates that NightNet can achieve better

reconstruction performance with relatively lower model complexity and computation."

Comment #6: Optimize the visualization effect of Figure 8: the global NTL distribution pattern is unclear, it is recommended to add local enlarged views or adjust the color matching to enhance the readability of spatial distribution characteristics; in addition, supplement the spatial distribution maps of the original DMSP and NPP-VIIRS data (especially local enlarged views) for comparison, which can help readers intuitively identify the differences between the reconstructed product and the original multi-source data.

Response: Thanks for the suggestion. In the revised manuscript, we improved the visualization of Fig. 8 to enhance the readability of the global NTL distribution pattern. Specifically, we adjusted the color scheme of Fig.8 (a) to highlight spatial variations and added enlarged local views to present spatial details. In addition, we supplemented the comparative spatial distribution maps of the original DMSP and NPP-VIIRS data with corresponding local zoom-in views, for a more intuitive comparison. To quantitatively demonstrate the effectiveness of the proposed approach in mitigating saturation and blooming effects, we added a comparison between the raw DMSP and simulated VIIRS at the left panel of Fig. 8. These revisions have been incorporated into the updated Fig. 8 (pages 15-16, lines 478-508).

Revised version of Fig. 8 in the updated manuscript:

"

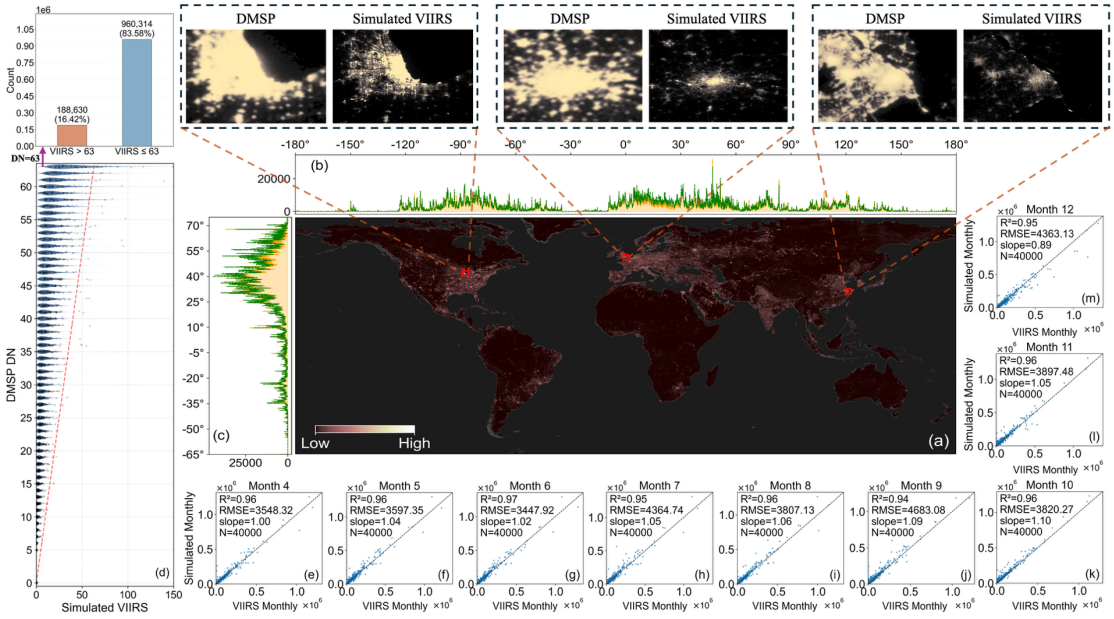

Figure 8. The simulated VIIRS-like data. **(a)** The generated global NTL intensity in 2012. **(b)** The longitudinal and **(c)** latitudinal sum of VIIRS NTL (orange) and Predicted VIIRS (green) with 1° bin (unit: nW cm^{-2} sr^{-1}). **(d)** Distribution of simulated VIIRS NTL across DMSP DN levels. **(e)** to **(m)** illustrate the city-level prediction errors of the total monthly VIIRS-like NTL from April to December 2012 at the global scale (unit: nW cm^{-2} sr^{-1}).

To evaluate the spatial consistency and reconstruction accuracy of the generated dataset at the global scale, we conducted a visual assessment using the reconstructed annual mean VIIRS-like product for 2012 and a comparative analysis of the monthly reconstructions from April to December 2012. The middle panel of Fig. 8 shows the model-generated global NTL intensity in 2012, with

aggregated radiance distributions along the longitudinal and latitudinal dimensions. Panel (a) shows the spatial distribution of the reconstructed NTL intensity, expressed in nW cm^{-2} sr^{-1}, revealing the global patterns of major cities and urban corridors. This distribution clearly delineates the spatial extent of human activity across all continents. Panels (b) and (c) illustrate the one-degree binned total radiance of the original VIIRS observations shown in orange and the predicted results shown in green along the longitudinal and latitudinal directions, respectively. The two curves exhibit strong agreement, particularly in densely urbanized latitudinal zones. These results indicate that the reconstructed data successfully reproduce the global-scale spatial patterns of the original VIIRS product.

Panel (d) further quantifies the radiometric relationship between the reconstructed data and the original DMSP digital number values. Unlike the pronounced saturation plateau at high DN levels in the raw DMSP data, the reconstructed VIIRS-like NTL exhibits a more continuous radiometric response, effectively mapping saturated values into a broader radiance range. This improvement is supported by the statistics in the upper-left panel, where 16.42% of pixels with DMSP DN = 63 are reassigned to simulated VIIRS-like values greater than 63, indicating that a substantial portion of saturated pixels is released from the original upper limit. For visual comparison, representative regions in North America, Europe, and Asia are selected, and all qualitative examples in the top panels are displayed within a fixed range of 0–63 to ensure consistency with the original DMSP scale. Under this unified visualization, the simulated VIIRS-like NTL shows reduced overglow, clearer light boundaries, and enhanced spatial detail, further demonstrating its effectiveness in mitigating blooming effects. As our MVNL dataset is designed to provide a monthly enhanced reference, the accuracy of the monthly reconstructions was further evaluated by comparing simulated and observed data for overlapping months at the city scale. Panels (e) to (m) in Fig. 8 show scatter plot comparisons between the simulated monthly results and the EOG monthly VIIRS observations from April to December 2012. The results demonstrate high radiance consistency at the city scale between the reconstructed and observed data. For all overlapping months, the regression slopes are close to unity, and the coefficients of determination exceed 0.94, while the city-level RMSE values range from 3447 to 4683, indicating relatively low errors."

Comment #7: It is suggested (not mandatory) to add a pixel-scale accuracy comparison across different regions in the precision validation part. NTL data quality and precision are inherently different in different regions (e.g., DMSP saturation leads to lower precision in highly urbanized areas, and precision differences may also exist across latitudes/geographical regions). Pixel-scale regional precision assessment can help users apply this 500 m high-resolution product more scientifically and objectively, and better reflect the advantages of the high-resolution product proposed in this study.

Response: Thank you for this suggestion. We agree that pixel-scale regional accuracy assessment is important for understanding spatial heterogeneity in NTL data quality. In current revision, we have not included an additional set of region-specific pixel-scale comparisons. Instead, we rely on the existing pixel-level evaluations across different continents (Fig. 10) and representative countries (Figs. 11 and 12), which include both highly urbanized regions affected by saturation and less-developed regions with lower lighting intensity. These regions also span a range of latitudes, thereby partially reflecting regional differences in model performance. While we acknowledge that a more explicit regional stratification could provide further insights, we believe the current validation

already provides a reasonably comprehensive assessment. We will consider incorporating more detailed region-specific evaluations in future work.

Comment #8: If there are other existing similar NTL products, adding a comparative analysis with these products can further highlight the advantages of this study's product. Relatively speaking, for manuscripts focusing on data product development, the analysis of the correlation between NTL and population, economic activities, energy consumption, etc., may not be so important (if the manuscript has page limitations).

Response: Thank you. At present, there are no directly comparable long-term monthly NTL products at 500 m resolution with similar temporal coverage, which limits the feasibility of a direct monthly comparison. To address this limitation, we performed several complementary analyses in the revised manuscript. **First**, we compared the proposed dataset with currently available annual NTL products, as shown in Fig. 23 (corresponding to Fig. 22 in the original manuscript), to evaluate its long-term temporal continuity and consistency relative to existing products. **Second**, we further compared the relationships between annual total NTL intensity and macro-scale socioeconomic indicators, including GDP and population, across multiple datasets, as shown in Fig. 25 (Fig. 24 in the original manuscript). This comparison provides an additional perspective on the performance of the proposed dataset relative to existing annual products in representing large-scale socioeconomic patterns. **Third**, because monthly socioeconomic statistics are available for some representative countries, we also examined the relationship between the reconstructed monthly NTL data and monthly GDP data, such as those for Mexico and the United Kingdom (Fig. 26, corresponding to Fig. 25 in the original manuscript), to assess the ability of the dataset to capture monthly economic dynamics. Together, these analyses further support the reliability and applicability of the proposed dataset and provide a reasonable alternative in the absence of directly comparable monthly 500 m NTL products.

Referee #3:

Comments:

This paper presents a valuable and well-constructed dataset that bridges DMSP-OLS and NPP-VIIRS observations to produce a long-term, monthly, and consistent nighttime light (NTL) product. The effort to reconstruct VIIRS-like monthly data from historical DMSP records is important, and I believe this dataset will be highly useful for a wide range of socioeconomic and urban studies. The manuscript is generally well written, and the results are promising. I have several minor suggestions that could further strengthen the paper:

Comment #1: The manuscript mentions the saturation and blooming effects in DMSP data. It would be helpful to provide quantitative evidence demonstrating how well saturation and blooming effects are mitigated compared to the raw DMSP data.

Response: Thank you for this helpful suggestion. In the revised manuscript, we have provided additional quantitative and qualitative evidence to demonstrate the mitigation of saturation and blooming effects from following aspects.

First, we supplemented a quantitative comparison between the original DMSP and simulated

VIIRS data for 2012 in Fig. 8(d). The results show that the proposed model effectively remaps the original 0–63 DMSP DN values into a broader radiometric range, both compressing and expanding them. The reconstructed VIIRS-like data are therefore no longer constrained by DMSP's limited dynamic range, indicating effective mitigation of saturation effects. In addition, the statistics shown in the upper-left panel of Fig. 8 further support this result, with 16.42% of pixels with DMSP DN = 63 reassigned to simulated VIIRS-like values greater than 63, providing additional quantitative evidence that saturated pixels are released from the original upper limit constraint.

Second, to illustrate the reduction of blooming effects, we added visual comparisons in three representative regions at the top of Fig. 8. All examples are displayed within the same 0–63 range to ensure direct visual comparability with the original DMSP data. Under this consistent setting, the reconstructed NTL data exhibit clearer boundaries, reduced overglow, and enhanced spatial detail.

Third, in the spatial validation (Section 5.1), we included additional comparisons for two representative regions in Fig. 21 and revised the related descriptions of Figs. 19 and 20. Specifically, Figs. 19 and 20 present side-by-side comparisons of DMSP and reconstructed VIIRS-like data for Beijing and Shanghai across representative years and months, enabling direct visualization of seasonal and interannual variations. In Beijing, the reconstructed results exhibit clearer urban boundaries, reduced blooming, and more stable seasonal variation than the original DMSP data. In Shanghai, the reconstructed results not only reduce blooming effects but also alleviate saturation in highly illuminated urban cores, leading to a more differentiated representation of brightness gradients and urban expansion. Fig. 21 further provides temporal comparisons of total NTL intensity in these two cities. In regions strongly affected by blooming, such as Beijing, the reconstructed data suppress anomalously inflated bright areas and produce a more stable temporal pattern. In regions more strongly affected by saturation, such as Shanghai, the reconstructed data better capture the continued growth of NTL, particularly after 2010. These additions provide more comprehensive evidence of the effectiveness of the proposed method in mitigating saturation and blooming.

"

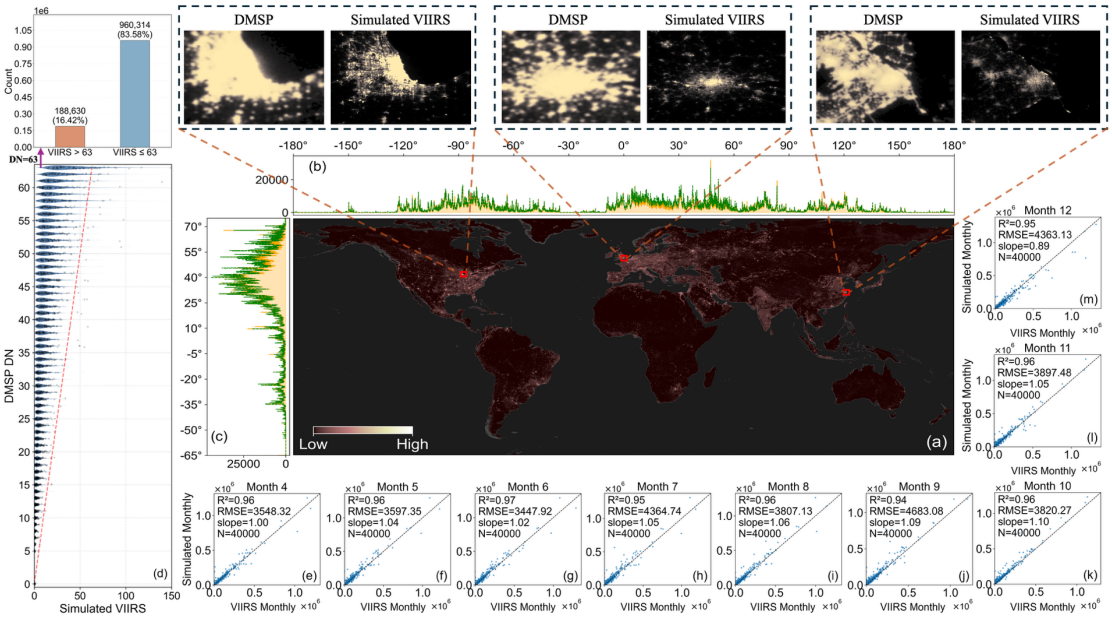

Figure 8. The simulated VIIRS-like data. **(a)** The generated global NTL intensity in 2012. **(b)** The longitudinal and **(c)** latitudinal sum of VIIRS NTL (orange) and Predicted VIIRS (green) with 1° bin (unit: nW cm^{-2} sr^{-1}). **(d)**

Distribution of simulated VIIRS NTL across DMSP DN levels. **(e)** to **(m)** illustrate the city-level prediction errors of the total monthly VIIRS-like NTL from April to December 2012 at the global scale (unit: nW cm^{-2} sr^{-1})."

About Figs. 19 and 20:

"To characterize the long-term spatiotemporal evolution of NTL captured by the constructed dataset, reconstructed VIIRS-like NTL distributions for two representative developing megacities, Beijing and Shanghai, together with the corresponding DMSP observations, are presented for different months and key years during 1992–2012, as shown in Figs. 19 and 20. In both figures, representative years are arranged in columns and different months in rows, allowing the seasonal variability and interannual evolution of urban NTL to be directly visualized while enabling a side-by-side comparison between the original DMSP data and the reconstructed VIIRS-like results. In Beijing (Fig. 19), NTL data in the early years are mainly concentrated within the urban core, with limited spatial extent. Over time, both brightness intensity and illuminated coverage increase continuously and gradually expand toward peripheral areas, revealing clear signatures of urban expansion and functional spillover. Compared with the original DMSP observations, the reconstructed VIIRS-like results exhibit clearer boundaries, reduced blooming effects, and improved spatial separability. The spatial configuration remains relatively stable across months, indicating that seasonal variation is mainly reflected in brightness changes rather than in fundamental changes in spatial structure. In Shanghai (Fig. 20), the spatial pattern is characterized by stronger high-intensity aggregation, with a bright urban core already evident in the early years, followed by rapid outward expansion along major urban corridors and toward coastal areas in later years, resulting in progressively more continuous and compact NTL distributions. Compared with Beijing, Shanghai exhibits higher overall brightness levels and faster spatial expansion in most months, reflecting a more concentrated urban structure and stronger economic activity. The comparison with the original DMSP images further shows that the reconstructed VIIRS-like NTL not only suppresses blooming effects but also alleviates saturation in highly illuminated areas.

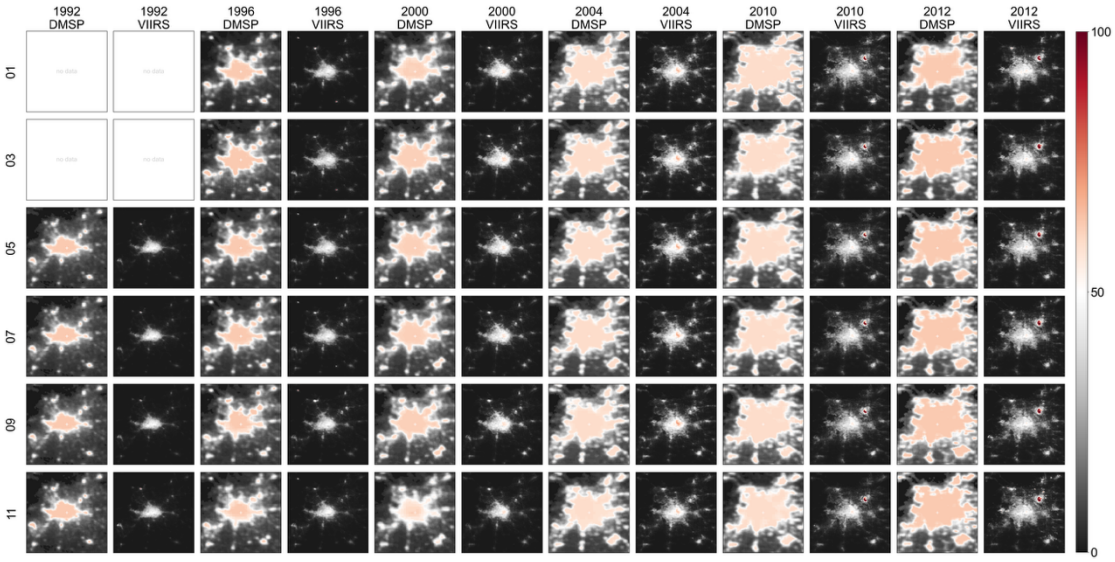

Figure 19. Seasonal and interannual spatial patterns of DMSP and reconstructed VIIRS-like NTL in Beijing from 1992 to 2012.

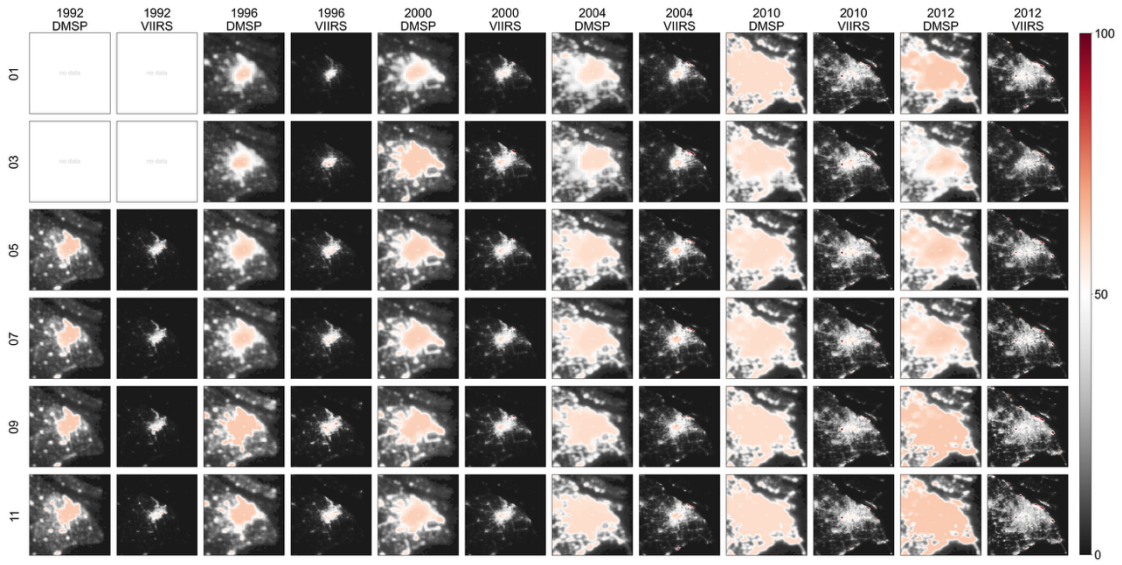

Figure 20. Seasonal and interannual spatial patterns of DMSP and reconstructed VIIRS-like NTL in Shanghai from 1992 to 2012."

About Fig. 21:

"A quantitative assessment of the seasonal and interannual dynamics of total NTL intensity was further conducted for Beijing and Shanghai, as shown in Fig. 21. The temporal profiles reveal clear and consistent intra-annual fluctuations in both cities, indicating that the reconstructed VIIRS-like data effectively preserve seasonal variability while also reflecting long-term interannual growth. In Beijing (Fig. 21(a)), the simulated VIIRS-like series exhibits a smoother temporal trajectory than the original DMSP totals, with reduced abnormal peaks and compressed excessively bright values, suggesting that blooming effects have been substantially mitigated. In Shanghai (Fig. 21(b)), the reconstructed MVNL series not only shows a similar improvement in suppressing blooming effects but also exhibits consistently higher total light values than the corresponding DMSP DN totals after 2010. This pattern suggests that the saturation limitation in the original DMSP observations has been effectively alleviated, enabling the reconstructed data to more accurately capture the ongoing increase in NTL intensity associated with rapid urban growth.

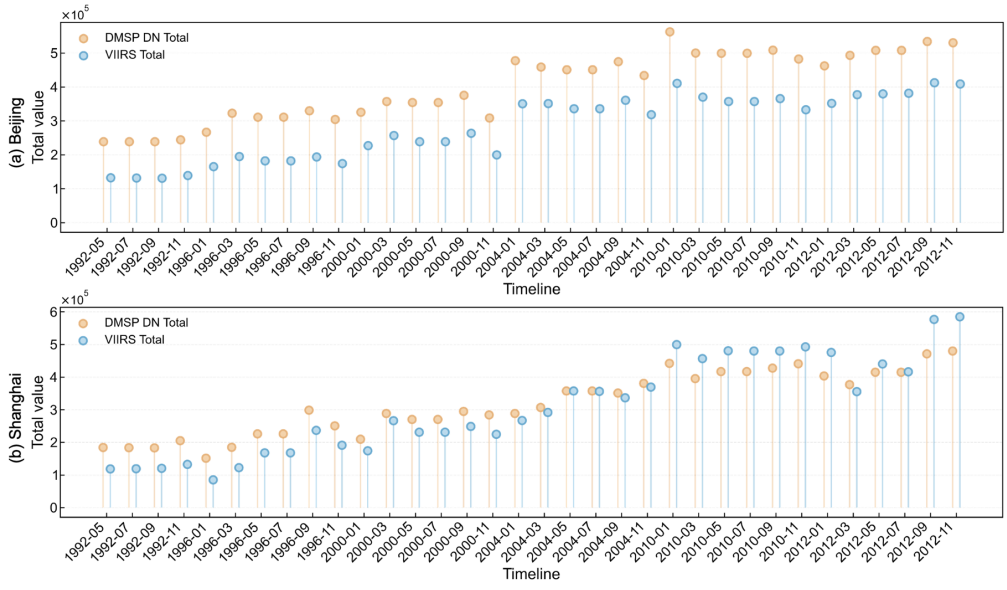

Figure 21. Seasonal and interannual NTL comparison from DMSP and simulated VIIRS in representative cities: **(a)**

Beijing and **(b)** Shanghai."

Comment #2: Please ensure consistent use of the term “nighttime light (NTL)” throughout the manuscript (e.g., around Line 310).

Response: Thank you for this careful observation. In the revised manuscript, we have checked and standardized the terminology throughout the text to ensure consistent use of "nighttime light (NTL)". Relevant instances have been corrected accordingly.

Comment #3: The discussion of seasonal variation (e.g., Figures 19 and 20) is informative, but could be strengthened by including quantitative metrics to more clearly demonstrate how well seasonal dynamics are captured. In addition, a comparison with the seasonal patterns derived from monthly DMSP data would be valuable, as it could further highlight the improvements and added value of the proposed dataset.

Response: Thank you for this suggestion. In the revised manuscript, we further strengthened the analysis of seasonal variation in two aspects. **First**, we added quantitative temporal comparisons for two representative regions in Fig. 21. The results show that the reconstructed dataset preserves clear intra-annual fluctuation patterns while providing a more stable and coherent representation of seasonal variability than the original DMSP data. In Beijing, the comparison suggests that blooming effects are substantially reduced in the reconstructed series, as reflected by the suppression of anomalously inflated light totals and a more consistent seasonal pattern. In Shanghai, the reconstructed results not only reduce blooming but also alleviate saturation. Specifically, the simulated VIIRS-like light totals are consistently higher than the corresponding DMSP DN totals after 2010, suggesting that the original 0–63 DMSP range is insufficient to capture nighttime light dynamics in this rapidly developing, highly illuminated region. **Second**, we revised the descriptions of Figs. 19 and 20, and supplemented the comparison between the original DMSP observations and the reconstructed VIIRS-like results for Beijing and Shanghai across different months and representative years. These visual comparisons further highlight the improvements in seasonal continuity, boundary clarity, blooming suppression, and spatial detail. Together, these additions provide more comprehensive evidence that the proposed dataset offers a clearer and more temporally coherent representation of seasonal dynamics than the original monthly DMSP observations.

About Fig. 21:

"A quantitative assessment of the seasonal and interannual dynamics of total NTL intensity was further conducted for Beijing and Shanghai, as shown in Fig. 21. The temporal profiles reveal clear and consistent intra-annual fluctuations in both cities, indicating that the reconstructed VIIRS-like data effectively preserve seasonal variability while also reflecting long-term interannual growth. In Beijing (Fig. 21(a)), the simulated VIIRS-like series exhibits a smoother temporal trajectory than the original DMSP totals, with reduced abnormal peaks and compressed excessively bright values, suggesting that blooming effects have been substantially mitigated. In Shanghai (Fig. 21(b)), the reconstructed MVNL series not only shows a similar improvement in suppressing blooming effects but also exhibits consistently higher total light values than the corresponding DMSP DN totals after 2010. This pattern suggests that the saturation limitation in the original DMSP observations has been

effectively alleviated, enabling the reconstructed data to more accurately capture the ongoing increase in NTL intensity associated with rapid urban growth.

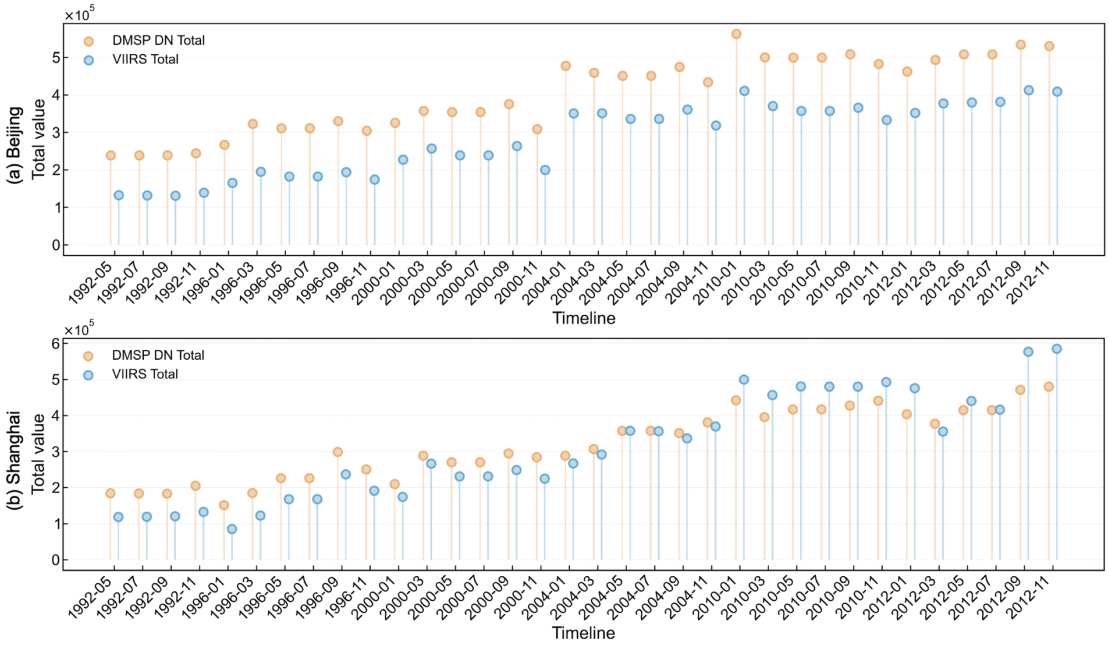

Figure 21. Seasonal and interannual NTL comparison from DMSP and simulated VIIRS in representative cities: **(a)** Beijing and **(b)** Shanghai."

About Figs. 19 and 20:

"To characterize the long-term spatiotemporal evolution of NTL captured by the constructed dataset, reconstructed VIIRS-like NTL distributions for two representative developing megacities, Beijing and Shanghai, together with the corresponding DMSP observations, are presented for different months and key years during 1992–2012, as shown in Figs. 19 and 20. In both figures, representative years are arranged in columns and different months in rows, allowing the seasonal variability and interannual evolution of urban NTL to be directly visualized while enabling a side-by-side comparison between the original DMSP data and the reconstructed VIIRS-like results. In Beijing (Fig. 19), NTL data in the early years are mainly concentrated within the urban core, with limited spatial extent. Over time, both brightness intensity and illuminated coverage increase continuously and gradually expand toward peripheral areas, revealing clear signatures of urban expansion and functional spillover. Compared with the original DMSP observations, the reconstructed VIIRS-like results exhibit clearer boundaries, reduced blooming effects, and improved spatial separability. The spatial configuration remains relatively stable across months, indicating that seasonal variation is mainly reflected in brightness changes rather than in fundamental changes in spatial structure. In Shanghai (Fig. 20), the spatial pattern is characterized by stronger high-intensity aggregation, with a bright urban core already evident in the early years, followed by rapid outward expansion along major urban corridors and toward coastal areas in later years, resulting in progressively more continuous and compact NTL distributions. Compared with Beijing, Shanghai exhibits higher overall brightness levels and faster spatial expansion in most months, reflecting a more concentrated urban structure and stronger economic activity. The comparison with the original DMSP images further shows that the reconstructed VIIRS-like NTL not only suppresses blooming effects but also alleviates saturation in highly illuminated areas.

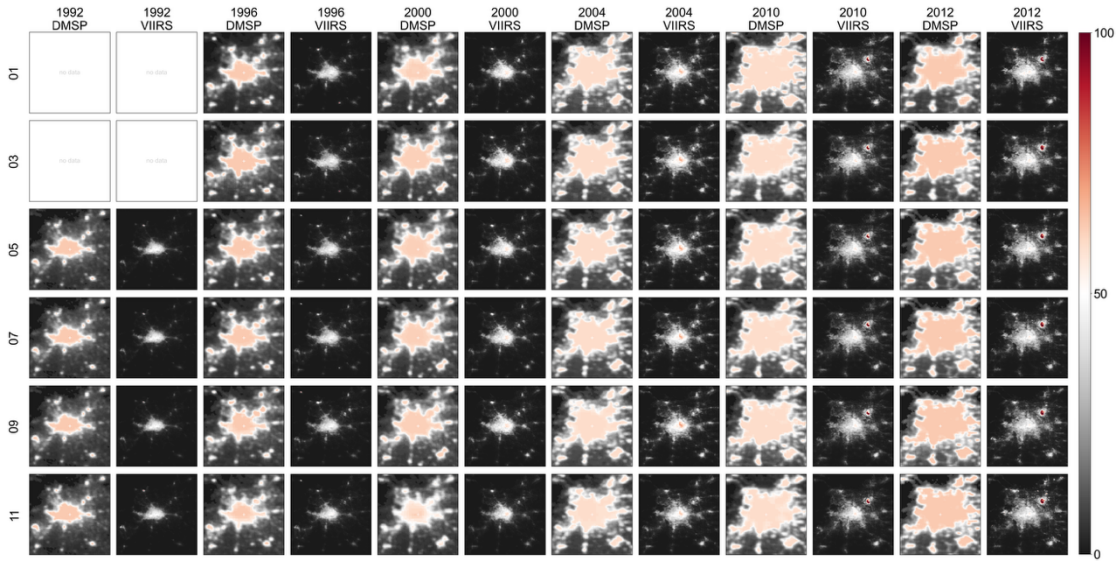

Figure 19. Seasonal and interannual spatial patterns of DMSP and reconstructed VIIRS-like NTL in Beijing from 1992 to 2012.

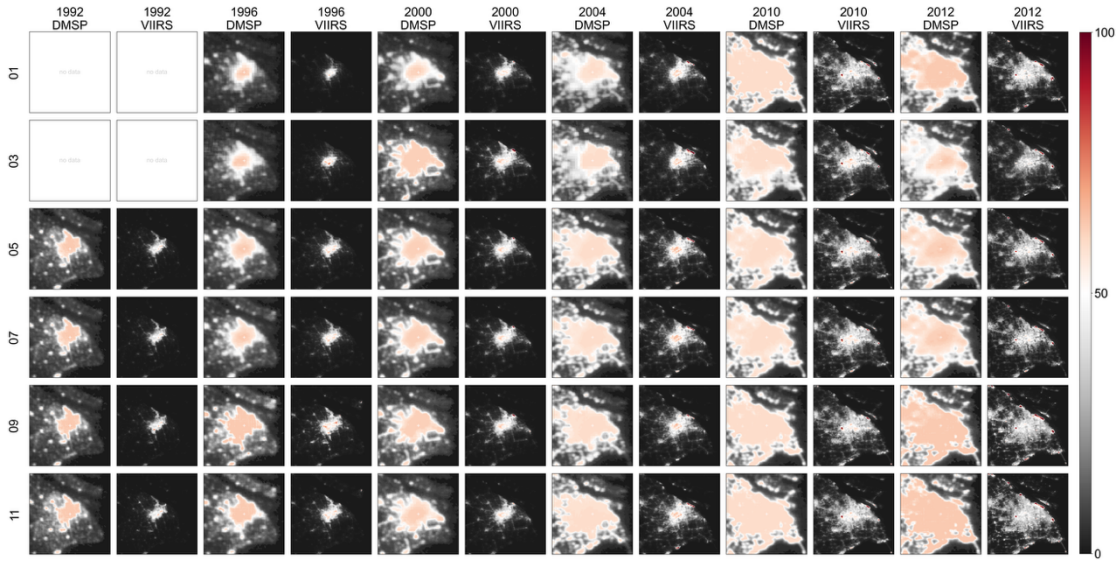

Figure 20. Seasonal and interannual spatial patterns of DMSP and reconstructed VIIRS-like NTL in Shanghai from 1992 to 2012."

Comment #4: The model is trained using data from 2013, while overlapping data are available for both 2012 and 2013. Please clarify why 2012 was not included. A comparison between models trained on different years (e.g., 2012 vs. 2013) could also help demonstrate the robustness of the approach.

Response: Thank you for this insightful comment. Although part of the overlapping period, 2012 was not used for model training because the EOG monthly VIIRS data began only in April 2012. As a result, the corresponding annual composite cannot adequately capture the full-year variation in nighttime light, which may introduce bias in cross-sensor model learning. In contrast, 2013 provides complete and consistent observations from both DMSP and NPP-VIIRS, making it more suitable for establishing the cross-sensor mapping.

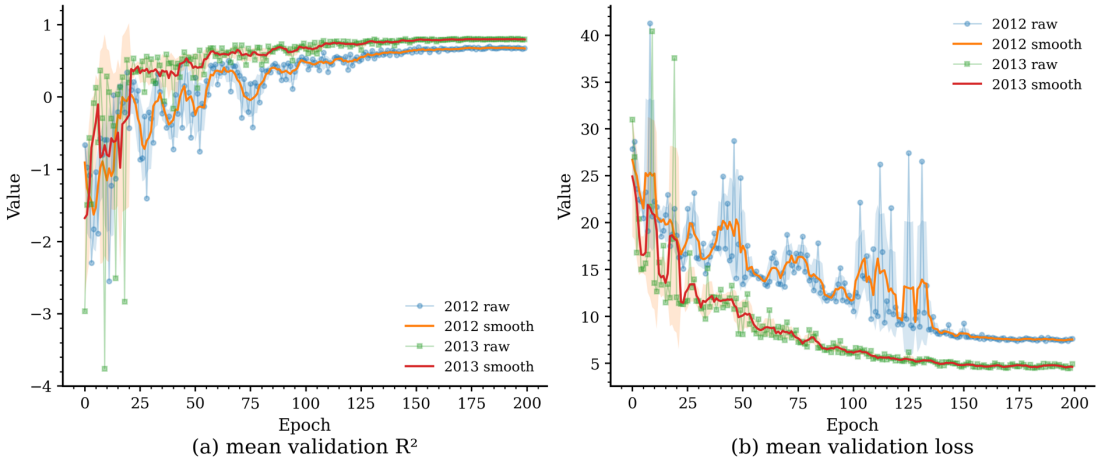

Figure A1. Performance of models trained using the data from 2012 and 2013, respectively.

To address this issue, we conducted additional comparative experiments by training the model using 2012 and 2013 data under the same settings. The quantitative results (Fig. A1) show that the model trained on 2012 data yields a lower validation R^2 of 0.7008, which is 10.70% lower than that obtained with 2013 data. In addition, the point-wise validation loss is consistently higher when 2012 is used as the training year. These results further support the rationale for selecting 2013 for model training. Considering the current length of the manuscript, we have not included the additional comparison figure in the revised paper. Instead, we have strengthened the discussion in the data selection section to explain why 2013 was chosen for model training rather than 2012.

Statement (on page 5, lines 166-169):

"Cross-sensor calibration in this study relied on NPP-VIIRS NTL observations from 2013, when both NPP-VIIRS and DMSP-OLS were in operation, and complete annual observations were available from both sensors. Although 2012 was also an overlapping year, the monthly NPP-VIIRS record began only in April, making its annual composite less representative of full-year NTL variation and therefore less suitable for model calibration."

Comment #5: The proposed network consists of three major functional modules; the overall architecture appears relatively complex. While the design is technically sound, it would be helpful to include, in Section 3.2, a discussion comparing the proposed model with simpler baseline networks (e.g., conventional CNN-based architectures). Such comparisons would help clarify the rationale for adopting the current design and its added value.

Response: Thanks for the comment. In the revised manuscript, we have added comparative experiments with several representative CNN-based baseline networks, including FCN, UNet, DeepLab v3+, and HRNet, better to demonstrate the rationale and effectiveness of the proposed architecture. The results show that the proposed NightNet achieves the best overall performance among the compared methods, with a PSNR of 52.42, an SSIM of 0.9930, and an R^2 of 0.8078. In particular, although some baseline models, such as DeepLab v3+, also achieve relatively strong performance, NightNet still yields substantial improvements, especially in R^2, indicating stronger consistency with the target VIIRS-like radiometric characteristics. From a model design perspective, these improvements are closely related to NightNet's dedicated functional modules. The multi-level deformable alignment and fusion module helps address spatial misalignment and heterogeneous feature inconsistency between DMSP and auxiliary data, the hierarchical contextual feature

enhancement module strengthens the recovery of complex urban structures and illumination gradients, and the multi-task synergistic learning module introduces additional structural constraints to stabilize training and improve generalization. Therefore, the proposed architecture is not only empirically more effective but also more suitable for solving the key challenges of cross-sensor VIIRS-like NTL reconstruction.

In addition, the comparison also shows that the improved performance is not solely due to increased model complexity. For example, DeepLab v3+ has significantly higher model parameters (40.34M) than the proposed model (9.21M), yet yields lower reconstruction accuracy. This demonstrates that the proposed architecture achieves a better balance between model complexity and performance. These results quantitatively demonstrate the added value of the proposed multi-module design, and corresponding descriptions have been incorporated into Section 4.1 (pages 14 and 15, lines 467–477 in the revised manuscript).

Supplementary experiments:

"**Table 1.** Quantitative comparison of the proposed method with baseline networks

Method	Params. (M)	FLOPs (G)	PSNR	SSIM	R^2
FCN	1.18	1.10	46.89	0.9676	0.3817
UNet	0.79	51.49	46.37	0.9623	-
DeepLabv3+	40.34	17.26	50.44	0.9877	0.4878
HRNet	18.80	7.30	46.42	0.9620	-
NightNet	9.21	9.80	52.42	0.9930	0.8078

A comparison between NightNet and several widely used representative baseline networks, including FCN (Long et al., 2015), UNet (Ronneberger et al., 2015), DeepLabv3+ (Chen et al., 2018), and HRNet (Wang et al., 2021), was conducted to evaluate the effectiveness of the proposed architecture and clarify the rationale for its design. The quantitative results in terms of model complexity and reconstruction performance are presented in Table 1. As shown, our NightNet achieves the best overall performance, with the highest PSNR (52.42), SSIM (0.9930), and R^2 (0.8078), indicating superior reconstruction accuracy and structural consistency. Although some baseline models, such as DeepLab v3+, also show relatively strong performance, their results remain inferior to those of NightNet. Moreover, the DeepLab v3+ model has more model parameters (40.34M parameters) than NightNet (9.21M), yet yields lower reconstruction accuracy. The result indicates that NightNet can achieve better reconstruction performance with relatively lower model complexity and computation."

We have carefully revised the manuscript and implemented the necessary changes throughout the paper. For clarity, all modifications have been highlighted in red in the revised version rather than listed separately here.

We appreciate the time and effort that the Editors and Referees devoted to evaluating our manuscript, and we hope that the revised version meets with your approval.

Thank you again for your valuable comments and thoughtful suggestions.